Available online at www.sciencedirect.com
SCIENCE DIRECT®
PERGAMON
International Journal of Multiphase Flow 29 (2003) 1605–1624
International Journal of Multiphase Flow
www.elsevier.com/locate/ijmulflow

Power law and composite power law friction factor correlations for laminar and turbulent gas–liquid flow in horizontal pipelines

F. García [a], R. García [a], J.C. Padrino [b], C. Mata [b], J.L. Trallero [b], D.D. Joseph [c,*]

[a] *School of Mechanical Engineering and Fluid Mechanics Institute, Central University of Venezuela, Caracas 1051, Venezuela*
[b] *PDVSA-Intevep, Los Teques 1201, Venezuela*
[c] *Department of Aerospace Engineering and Mechanics, University of Minnesota, 107 Akerman Hall, 110 Union Street SE, Minneapolis, MN 55455, USA*

Received 20 September 2002; received in revised form 24 June 2003

Abstract

Data from 2435 gas–liquid flow experiments in horizontal pipelines, taken from different sources, including new data for heavy oil are compiled and processed for power law and composite power law friction factor correlations. To our knowledge this is the largest database so far published in the literature; it includes the widest range of operational conditions and fluid properties for two-phase friction factor correlations. Separate power laws for laminar and turbulent flows are obtained for all flows in the database and also for flows sorted by flow pattern. Composite analytical expressions for the friction factor covering both laminar and turbulent flows are obtained by fitting the transition region between laminar and turbulent flow with logistic dose curves. Logistic dose curves lead to rational fractions of power laws which reduce to the power laws for laminar flow when the Reynolds number is low and to turbulent flow when the Reynolds number is large. The Reynolds number appropriate for gas–liquid flows in horizontal pipes is based on the mixture velocity and the liquid kinematic viscosity. The definition of the Fanning friction factor for gas–liquid flow used in this study is based on the mixture velocity and density. Error estimates for the predicted vs. measured friction factor together with standard deviation for each correlation are presented. The correlations in this study are compared with previous correlations, homogeneous models and mechanistic models most commonly used for gas–liquid flow in pipelines. Since different authors use different definitions for friction factors and Reynolds numbers, comparisons of the predicted pressure drop for

* Corresponding author. Tel.: +1- 612-625-0309; fax: +1-612-626-1558.
E-mail address: joseph@aem.umn.edu (D.D. Joseph).

0301-9322/$ - see front matter
doi:10.1016/S0301-9322(03)00139-3

each and every data point in the database are presented. Our correlations predict the pressure drop with much greater accuracy than those presented by previous authors.

Keywords: Pipe flow; Friction-factor; Gas–liquid; Power law; Flow type

1. Introduction

The problem confronted in this study is how to predict the pressure drop in a horizontal pipeline. This problem is of great interest in many industries, especially in the oil industry. The approach taken in this work is based on recent applications of processing data from experiments (real or numerical) for power laws (Joseph, 2002; Patankar et al., 2001a,b, 2002; Wang et al., 2002; Pan et al., 2002; Viana et al., 2003; Mata et al., 2002).

Data from 2435 experiments, taken from different sources, have been compiled and processed. The data processed in this work include most of the data published in the prior literature plus new unpublished, and data for gas and heavy oil from PDVSA-Intevep.

Dimensionless pressure gradients are usually expressed as friction factors. The relation between pressure gradient and mass flux is expressed in dimensionless form as a relation between the friction factor and Reynolds number. In the engineering literature, one finds such plots of fluid response of one single fluid (one-phase) in the celebrated Moody diagram. The pipe roughness is an important factor in the Moody diagram; for turbulent flow in smooth pipes the data may be fit to the well-known power law of Blasius for which the friction factor increases with 0.25 power of Reynolds number. The Moody diagram may be partitioned into the three regions: laminar, transition and turbulent.

Here, we construct ''Moody diagrams'' for gas–liquid flows in horizontal pipelines in terms of a mixture Fanning friction factor and mixture Reynolds number selected to reduce the scatter in the data. The data is processed for power laws and a composite expression is found as a rational fraction of power laws which reduces to a ''laminar'' power law for low Reynolds numbers and a ''turbulent'' Blasius-like expression for large Reynolds numbers. We find that pipe roughness does not have a major effect on turbulent gas–liquid flow; the effects of interacting phases appear to dominate the effects of wall roughness.

It is well known that the pressure gradient depends on the flow type and prediction of the friction for each flow type can be found in the literature. Here, we depart from the path laid down by previous authors by creating composite correlations for each flow type and also for all the data without sorting according to flow type. Of course, the correlations for separate flow patterns are more accurate but possibly less useful than those for which previous knowledge of actual flow pattern is not required. A correlation for which a flow pattern is not specified is exactly what is needed in a field situation in which the flow patterns are not known.

The accuracy of the correlations developed in this paper is evaluated in two ways; by comparing predictions with the data from which the predictions are derived and by comparing the predictions of our correlations with predictions of other authors in the literature.

The comparison of our correlations with the literature is not conveniently carried in the friction factor vs. Reynolds number frame because different authors use different definitions of these

quantities. An unambiguous comparison is constructed by comparing predicted pressure gradients against the experiments in our database. We compared our predicted pressure gradients with those obtained from the correlations of Lockhart and Martinelli (1949), Dukler et al. (1964), Beggs and Brill (1973) and Ortega et al. (2001) as well as with the predictions of the homogeneous flow models of McAdams et al. (1942), Cicchitti et al. (1960), Beattie and Whalley (1982) and Ouyang (1998). We also compared our predicted pressure gradients with those obtained from the mechanistic models of Xiao et al. (1990), Ouyang (1998) and Padrino et al. (2002). Ouyang's models are for horizontal wells, which reduce to pipelines when the inflow from the reservoir is put to zero.

A comprehensive performance comparison between different models and correlations is achieved by means of the so-called modified relative performance factor (PF) proposed in this study. The performance factor is a statistical measure which allows models and correlations to be ranked for accuracy.

2. Dimensionless parameters

Due to the complexity of multiphase flow systems, it is not possible to obtain the governing dimensionless groups uniquely; various possibilities exist. For instance, Dukler et al. (1964) use one set, Beggs and Brill (1973) another set, Mata et al. (2002) another set and so on. In the present work, various combinations of dimensionless parameters were tried and judged by their success in reducing the root mean square percent relative error between the correlated and experimental values. **The dimensionless parameters** introduced by Mata et al. (2002) in a work on pressure drops in a flexible tube designed to model terrain variation are closely allied to this study and those dimensionless groups were found also to work best in our study.

The Fanning friction factor for the gas–liquid mixture f_M is defined as

$$f_M = \frac{(\Delta p/L)D}{2\rho_M U_M^2} \tag{1}$$

where the pressure drop per unit length $(\Delta p/L)$ is related to the wall shear stress $\tau_w = (D\Delta p/4L)$, D is the pipe diameter, $U_M = U_{SG} + U_{SL}$ is the mixture velocity which is defined in terms of the superficial gas velocity ($U_{SG} = 4Q_G/\pi D^2$) and the superficial liquid velocity ($U_{SL} = 4Q_L/\pi D^2$). Q_G and Q_L are the gas and liquid volumetric flow rates, respectively. The mixture density

$$\rho_M = \rho_L \lambda_L + \rho_G(1 - \lambda_L) \tag{2}$$

is a special kind of composite density weighted by the flow rate fraction, where λ_L is the liquid flow rate fraction.

$$\lambda_L = \frac{Q_L}{Q_L + Q_G} \tag{3}$$

ρ_G and ρ_L are the gas and liquid density, respectively.

The mixture Fanning friction factor f_M is correlated with a mixture Reynolds number defined by

$$\mathrm{Re} = \frac{U_M D}{v_L} \tag{4}$$

where $v_L = \mu_L/\rho_L$ is the kinematic viscosity of the liquid and μ_L is the dynamic viscosity; this definition acknowledges that the frictional resistance of the mixture is due mainly to the liquid.

The mixture friction factor f_M and the mixture Reynolds number Re definitions are greatly important in order to develop an appropriate correlation of the experimental data.

3. Universal (all flow patterns) composite (all Reynolds numbers) correlation for gas–liquid friction factors (FFUC)

Gas flow rate Q_G, liquid flow rate Q_L and differential pressure Δp measurements corresponding to 2435 experimental points taken from Intevep's databank, the Stanford University multiphase flow database (SMFD), and the database of the Tulsa University Fluid Flow projects (TUFFP) for gas–liquid flow in horizontal pipes were used in this study. These data are summarized in Tables 1–3. The columns in the tables are self explanatory except that "points" means the number of experiments, ε/D is the average size of pipe wall roughness over pipe diameter, FP means "flow pattern" and AN, DB, SL, SS and SW stand annular, dispersed bubble, slug, stratified smooth and stratified wavy flow, respectively.

A fraction of the experimental data (2060 experimental points) was used to calculate the experimental mixture friction factors. The points belonging to transition regions that come from Cabello's data (nine experimental points) and Ortega's data (32 experimental points) were excluded. The points that come from Rivero's data (74 experimental points), Eaton's data (51 experimental points) and SU199's data (209 experimental points) were excluded, because the pressure measurements had huge and unacceptable scatter for some points. The models and the correlations considered in Section 6, including ours, are tested against the entire database (2435 experimental points).

Fig. 1 shows the mixture friction factor f_M plotted against the mixture Reynolds number Re. In this figure, two clearly defined "laminar and turbulent" regions are observed, one region for values of Re less than 500 and the other one for values greater than 1000. Two reasonably good correlations were obtained fitting the data with power law correlations in both regions. However, the region between 500 and 1000 is not clearly defined.

A single equation (called composite) that can be used to predict the mixture friction factors for a wide range of gas and liquid flow rates, viscosity values, and different flow patterns was obtained fitting data with a logistic dose response curve applying a technique described by Barree (Patankar et al., 2002). The equation is given by

$$f_M = F_2 + \frac{(F_1 - F_2)}{\left(1 + \left(\frac{\mathrm{Re}}{t}\right)^c\right)^d} \tag{5}$$

where F_1 and F_2 are power laws defined as

$$F_1 = a_1 \mathrm{Re}^{b_1} \tag{6}$$

and

$$F_2 = a_2 \mathrm{Re}^{b_2} \tag{7}$$

Table 1
Intevep data

Source	Points	Fluids	μ_L [cP]	U_{SL} [m/s]	U_{SG} [m/s]	D [m]	ε/D	FP
Cabello et al. (2001)	26+9[a]	Air–kerosene	1	0.11–4.52	0.77–45.65	0.0508	0	AN DB SL SL–AN SL–DB
Mata et al. (2002)	31	Air–oil	100	0.11–1.49	0.06–3.43	0.0254	0	SL
Rivero et al. (1995)	74	Air–water Air–oil	1–200	0.02–0.19	0.61–11.89	0.0508	0	
Ortega et al. (2000)	50+20[a]	Air–oil	500	0.10–2.77	0.02–38.24	0.0508	0	AN DB SL SS SW SL–AN SL–DB SS–SL SW–AN
Ortega et al. (2001)	35+12[a]	Air–oil	1200	0.01–0.80	0.23–24.39	0.0508	0	AN SL SW SL–AN SW–AN SW–SL
Pereyra et al. (2001)[b]	94	Gas–HL	8–400	2.69–0.58	0.26–12.91	0.0779	5.9×10^{-4}	SL

[a] Transitions points.
[b] The live oil viscosity is reported, HL: Hydrocarbon liquid.

Table 2
Stanford data

Source	Points	Fluids	μ_L [cP]	U_{SL} [m/s]	U_{SG} [m/s]	D [m]	ε/D	FP
Alves (1954)	28	Air–oil	80	0.02–1.78	0.12–13.16	0.0266	1.7×10^{-3}	AN SL SW
Govier and Omer (1962)	57	Air–water	1	0003–1.53	0.05–16.57	0.0261	0	AN SL SS SW
Agrawal (1971)	19	Air–oil	5	0.01–0.06	0.11–6.16	0.0258	0	SS
Yu (1972)	15	Air–oil	5	0.10–0.32	0.07–0.62	0.0258	0	SL
Eaton (1966)	51	Gas–water	1	0.04–2.24	0.28–22.42	0.0508	8.0×10^{-4}	SL SS SW
Mattar (1973)	8	Air–oil	5	0.31–1.55	0.30–7.83	0.0258	0	SL
Aziz et al. (1974)	128	Air–oil	5	0.03–1.68	0.02–3.75	0.0258	0	DB SL
Companies[a]	141		3–19	0.07–6.26	0.32–63.44	0.0232	6.5×10^{-5}	
	146		3–19	0.07–5.96	0.28–57.09	0.0237	6.5×10^{-5}	AN
	61	Air–HL	1–25	0.02–3.40	0.10–24.05	0.0381	1.2×10^{-3}	SS
	209	Air–water	1	0.001–1.04	0.09–61.30	0.0455	0	SS
	470	Air–oil	3–15	0.03–7.25	0.04–69.56	0.0502	3.0×10^{-5}	SW
	131		3–22	0.03–7.10	0.16–59.52	0.0909	1.7×10^{-5}	
	156		3–20	0.07–6.07	0.11–24.47	0.1402	1.1×10^{-5}	

[a] Data sets are identified as: SU28, SU29, SU184–187, SU199, SU24, SU25 and SU26.

Table 3
Tulsa data

Source	Points	μ_L [cP]	U_{SL} [m/s]	U_{SG} [m/s]	D [m]	ε/D	FP
Andritsos (1986)	92	1–70	0.001–0.06	4.49–30.09	0.0252	0	AN
	111	1–80	0.001–0.19	4.29–29.51	0.0953		SL SS SW
Beggs (1972)	21	1	0.03–2.62	0.31–24.97	0.0254	0	AN DB SL
	22		0.02–1.60	0.37–15.12	0.0381		SS SW
Cheremisinoff (1977)	151	1	0.02–0.07	2.58–24.01	0.0635	0	SS SW
Kokal (1987)	10	8	0.03–0.06	1.18–11.51	0.0512	0	SS
	13		0.05–0.15	1.01–9.01	0.0763		SW
Mukherjee (1979)	44	1	0.03–3.40	0.23–24.06	0.0381	3.0×10^{-5}	AN SL SS SW

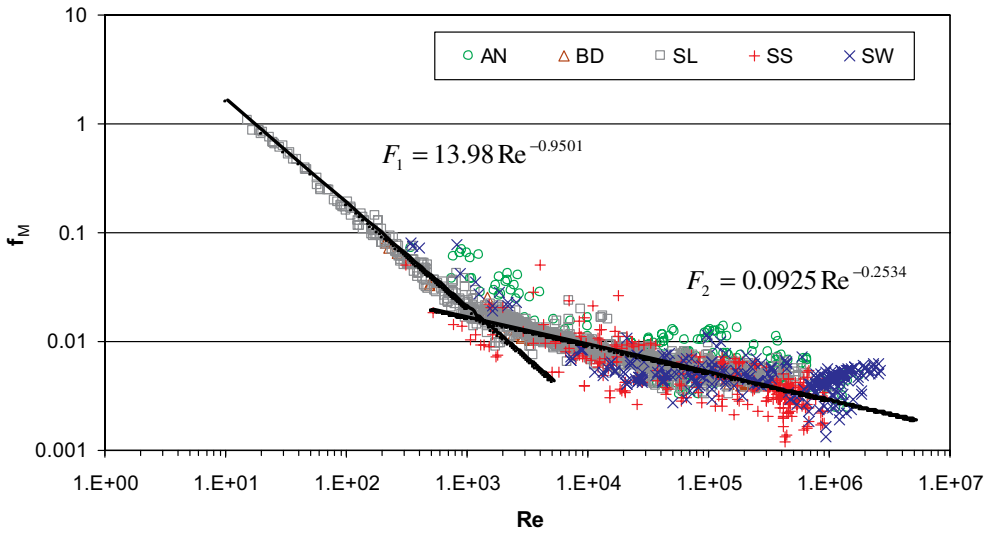

Fig. 1. Power law correlations for $Re < 500$ and $Re > 1000$.

c, d and t, are parameters obtained fitting Eq. (5) to the 2060 data points using the nonlinear optimization method of Microsoft® Excel Solver minimizing the residual mean square. The parameters a_1, b_1, a_2 and b_2 are obtained fitting the data with power law correlations in both regions.

Table 4
Parameters of the universal composite correlation for mixture Fanning friction factor

a_1	b_1	a_2	b_2	c	d	t
13.98	−0.9501	0.0925	−0.2534	4.864	0.1972	293

Eq. (5) implies that correlations in the entire range can be represented by power laws connected by transition regions (Patankar et al., 2002). The parameters c, d, t, a_1, b_1, a_2 and b_2 for this correlations are presented in Table 4.

The universal composite correlation for gas–liquid Fanning friction factor (FFUC) is then given by

$$f_M = 0.0925\mathrm{Re}^{-0.2534} + \frac{13.98\mathrm{Re}^{-0.9501} - 0.0925\mathrm{Re}^{-0.2534}}{\left(1 + \left(\frac{\mathrm{Re}}{293}\right)^{4.864}\right)^{0.1972}} \tag{8}$$

Fig. 2 shows the logistic dose response curve for the whole region.

The standard deviation of the correlated friction factor from the measured value was estimated to be 29.05% of the measured value.

It is important to point out that most of the points for turbulent flow in Fig. 2 fall in a relatively narrow band even though the roughness parameters for the pipes used to collect the data in the narrow band lie in a wide band, from 0 to 1.7×10^{-3} (ε/D in Tables 1–3). No single-phase turbulent flow like systematic behavior is noticed for data sets with similar relative roughness. It is possible that the disturbance due to interaction between one-phase and the other could overcome the relative roughness effect in two-phase flow dynamics. The influence of relative roughness in multiphase flow needs further study, since it seems to be not completely understood.

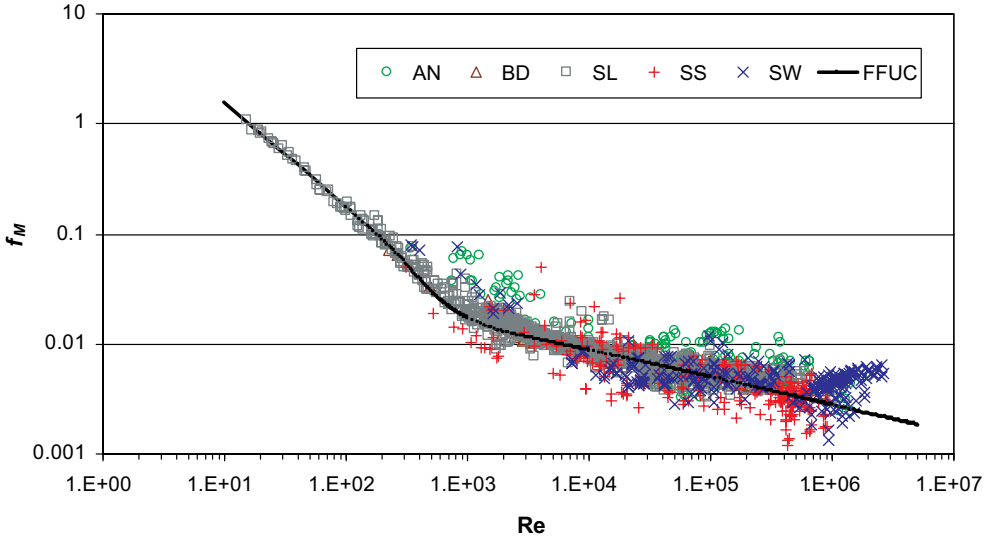

Fig. 2. Universal composite correlation (8).

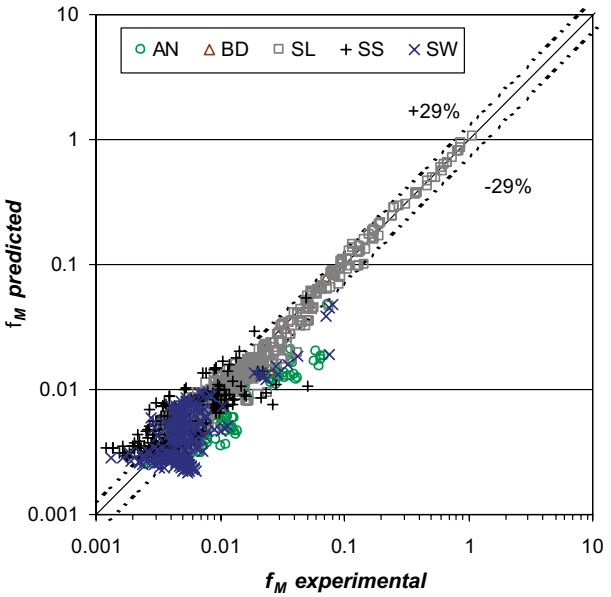

Fig. 3. Predicted mixture Fanning friction factor (8) vs. experimental mixture Fanning friction factor for the universal composite correlation.

The spread of the experimental data around the composite friction factor correlation (8) is shown in Fig. 3.

The correlation (8) has an average error of −4.27% and an average absolute error of 20.27%. 75.73% of the points (1560 points) are in the band between ±29%. The best agreements are obtained for slug and dispersed bubble flow data, with an average absolute error of 12.41% and 8.98%, respectively. The worst agreements are obtained for annular and stratified flow data, with an average absolute error of 38.65% and 34.57%, respectively.

4. Friction factor correlations sorted by flow pattern (FFPC)

We fit the data from 2060 experiments to power laws using the logistic dose curve fitting procedure described in Section 3 to obtain composite correlations. Each and every experiment was classified for flow type: 1316 slug flow SL, 40 dispersed bubble DB, 528 stratified flow ST and 176 annular flow AN types and composite correlations were created for each flow type. The parameters c, d, t, a_1, b_1, a_2 and b_2 of each correlation are presented in Table 5.

Figs. 4 and 5 show the logistic dose response curves for slug and dispersed bubble flow, respectively.

The composite correlations for slug flow and dispersed bubble flow are given by, respectively:

$$f_{\mathrm{M}} = 0.1067\mathrm{Re}^{-0.2629} + \frac{13.98\mathrm{Re}^{-0.9501} - 0.1067\mathrm{Re}^{-0.2629}}{\left(1 + \left(\frac{\mathrm{Re}}{293}\right)^{3.577}\right)^{0.2029}} \tag{9}$$

Table 5
Parameters of the gas–liquid friction factor correlations for each flow pattern

FP	a_1	b_1	a_2	b_2	c	d	t
SL	13.98	−0.9501	0.1067	−0.2629	3.577	0.2029	293
DB	13.98	−0.9501	0.1067	−0.2629	2.948	0.2236	304
ST	13.98	−0.9501	0.0445	−0.1874	9.275	0.0324	300
AN	3.671	−0.6257	0.0270	−0.1225	2.191	0.2072	10 000

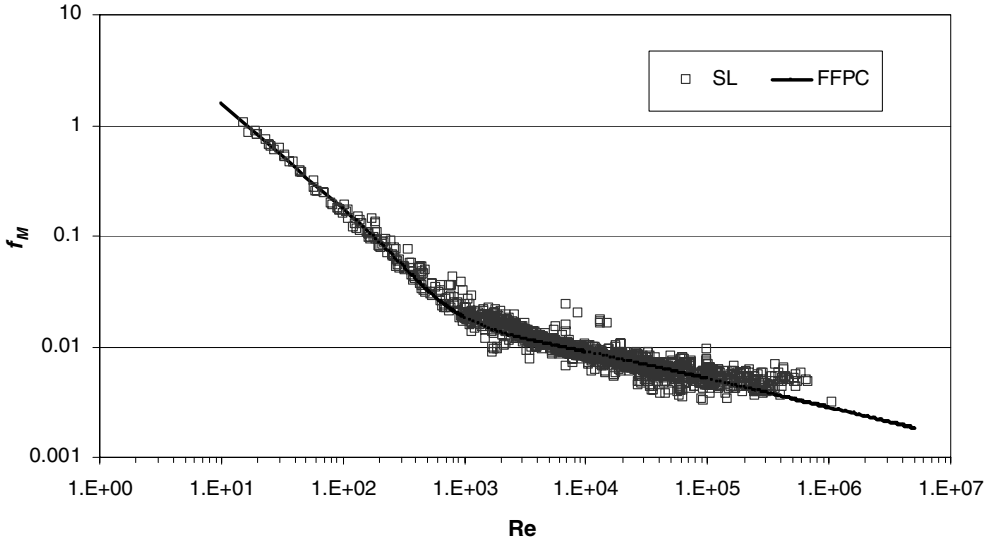

Fig. 4. Composite correlation (9) for slug flow.

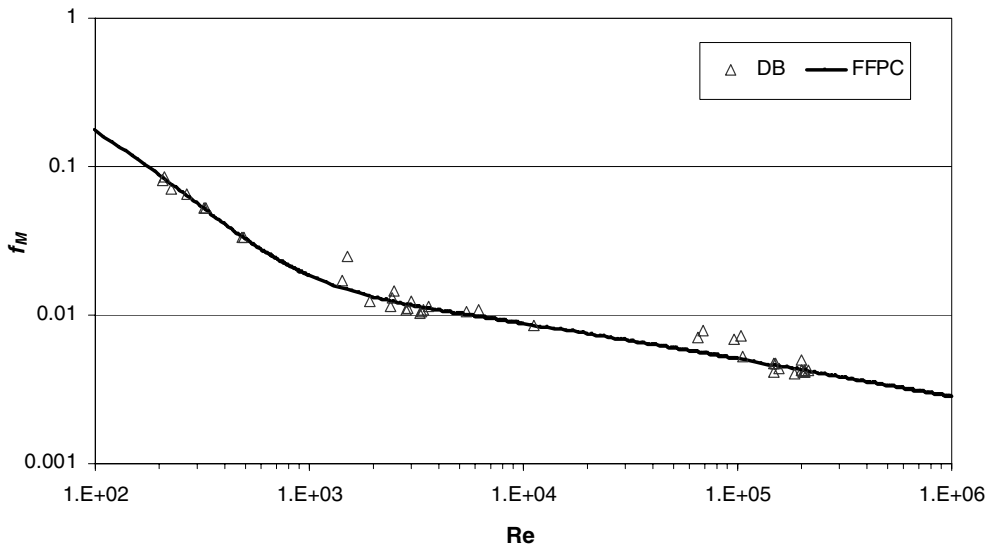

Fig. 5. Composite correlation (10) for dispersed bubble flow.

$$f_{\mathrm{M}} = 0.1067\mathrm{Re}^{-0.2629} + \frac{13.98\mathrm{Re}^{-0.9501} - 0.1067\mathrm{Re}^{-0.2629}}{\left(1 + \left(\frac{\mathrm{Re}}{304}\right)^{2.948}\right)^{0.2236}} \tag{10}$$

The standard deviations for the slug and dispersed bubble flow correlations of the correlated friction factors from the measured values were estimated to be 16.61% and 12.91% of the measured values, respectively. The spread of data around the correlation for slug flow is shown in Fig. 6. The slug flow friction factor correlation has an average error of −2.17% and an average absolute error of 11.99%. 75.30% of the points (991 points) are in the band between ±16.61%. The dispersed bubble flow friction factor correlation have an average error of −3.21% and an average absolute error of 8.32%. 82.50% of the points (33 points) are in the band between ±12.91%.

The logistic dose response curves for stratified flow and annular flow are shown in Figs. 7 and 8, respectively.

The composite correlations for stratified flow and annular flow are given by, respectively:

$$f_{\mathrm{M}} = 0.0445\mathrm{Re}^{-0.1874} + \frac{13.98\mathrm{Re}^{-0.9501} - 0.0445\mathrm{Re}^{-0.1874}}{\left(1 + \left(\frac{\mathrm{Re}}{300}\right)^{9.275}\right)^{0.0324}} \tag{11}$$

$$f_{\mathrm{M}} = 0.0270\mathrm{Re}^{-0.1225} + \frac{3.671\mathrm{Re}^{-0.6257} - 0.0270\mathrm{Re}^{-0.1225}}{\left(1 + \left(\frac{\mathrm{Re}}{10000}\right)^{2.191}\right)^{0.2072}} \tag{12}$$

The standard deviation of (11) for stratified flow is estimated as 38.40% of the measured value. The standard deviation (12) for annular flow is estimated to be 34.77% of the measured value. The

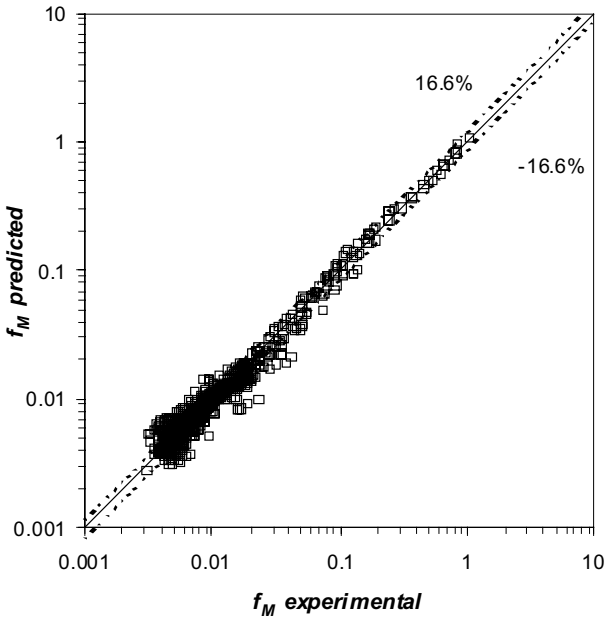

Fig. 6. Predicted mixture friction factor (9) vs. experimental mixture friction factor for slug flow.

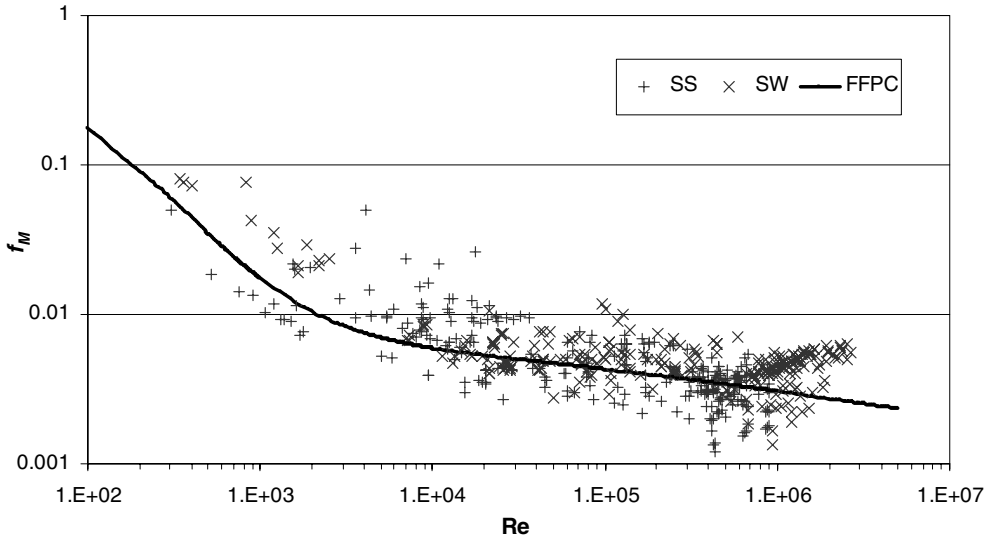

Fig. 7. Composite correlation (11) for stratified flow.

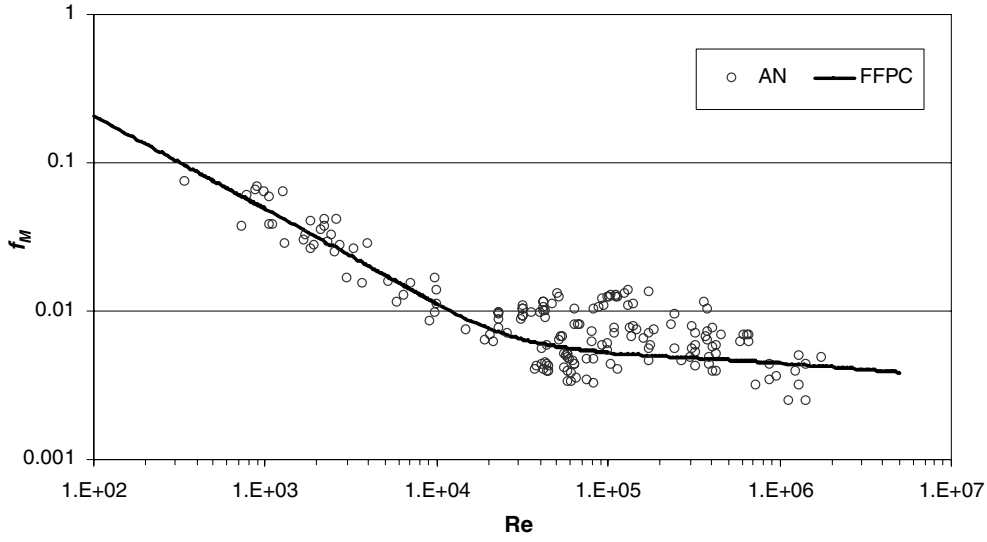

Fig. 8. Composite correlation (12) for annular flow.

average error for stratified flow is −6.80% and the average absolute error is 30.42%. Only 68.37% of the 520 points (361 points) are in the band between ±38.40%. The average error for annular flow is −7.36% and the average absolute error of 29.59%. However, only 64.20% of the 176 points (113 points) are in the band between ±34.77%.

5. Performance comparison of correlations and models for pressures drop from various sources against the data from 2435 experiments

The performance of predictions from our correlations for the pressure drop in the 2435 experiments in our database and models in the literature and our correlations will now be considered. Sources for the predictions are indexed as follows:

MHM (McAdams et al., 1942),
LMC (Lockhart and Martinelli, 1949),
CHM (Cicchitti et al., 1960),
DUC (Dukler et al., 1964),
BBC (Beggs and Brill, 1973),
BWHM (Beattie and Whalley, 1982),
XMM (Xiao et al., 1990),
OMM (Ouyang, 1998),
OHM (Ouyang, 1998),
ORC (Ortega et al., 2001),
PMM (Padrino et al., 2002),
FFPC (friction factor flow pattern correlations from Eqs. (9)–(12)),
FFUC (friction factor universal correlation from Eq. (8)).

The last C in the acronym stands for correlation, the MM stands for mechanistic model and HM stands for homogeneous model.

In the application of homogeneous flow models of McAdams et al. (1942), Cicchitti et al. (1960) and Beattie and Whalley (1982) we are only considering the frictional pressure gradient. The ϕ_L parameter, in the separated flow model of Lockhart and Martinelli (1949), is evaluated with the Chisholm (1967) correlation. The liquid holdup for Dukler et al. (1964) correlation is predicted from Bankoff's correlation as is suggested by Oballa et al. (1997).

The correlations developed in previous sections leading to FFPC and FFUC were developed by processing 2060 points. The remaining 375 data points, which were omitted in forming the correlations, were also classified for flow pattern so that those data points could be compared with predictors that specify flow type.

The comparison of the predictions of $\Delta p/L$ from different sources was accomplished by using a weighted measure PF which is a modification a measure recommended by Ansari et al. (1994) defined by

$$\mathrm{PF} = \frac{|E_1| - |E_{1\min}|}{|E_{1\max}| - |E_{1\min}|} + \frac{E_2 - E_{2\min}}{E_{2\max} - E_{2\min}} + \frac{E_3 - E_{3\min}}{E_{3\max} - E_{3\min}} + \frac{|E_4| - |E_{4\min}|}{|E_{4\max}| - |E_{4\min}|} + \frac{E_5 - E_{5\min}}{E_{5\max} - E_{5\min}} + \frac{E_6 - E_{6\min}}{E_{6\max} - E_{6\min}} \tag{13}$$

where E_1 is the average percent error, E_2 is average absolute percent error, E_3 is the standard deviation of the correlated value from the experimental value divided by the experimental value (root mean square percent error), E_4 is the average error, E_5 is average absolute error, and E_6 is the

standard deviation of the correlated value from the experimental value (root mean square error) which are defined as

$$E_1 = \left[\frac{1}{n} \sum_{i=1}^{n} \frac{(\Delta p_i/L)_{\text{pred}} - (\Delta p_i/L)_{\exp e}}{(\Delta p_i/L)_{\exp e}} \right] * 100 \tag{14}$$

$$E_2 = \left[\frac{1}{n} \sum_{i=1}^{n} \left| \frac{(\Delta p_i/L)_{\text{pred}} - (\Delta p_i/L)_{\exp e}}{(\Delta p_i/L)_{\exp e}} \right| \right] * 100 \tag{15}$$

$$E_3 = \left[\sqrt{\frac{1}{n-1} \sum_{i=1}^{n} \left(\frac{(\Delta p_i/L)_{\text{pred}} - (\Delta p_i/L)_{\exp e}}{(\Delta p_i/L)_{\exp e}} \right)^2} \right] * 100 \tag{16}$$

$$E_4 = \frac{1}{n} \sum_{i=1}^{n} (\Delta p_i/L)_{\text{pred}} - (\Delta p_i/L)_{\exp e} \tag{17}$$

$$E_5 = \frac{1}{n} \sum_{i=1}^{n} |(\Delta p_i/L)_{\text{pred}} - (\Delta p_i/L)_{\exp e}| \tag{18}$$

$$E_6 = \sqrt{\frac{1}{n-1} \sum_{i=1}^{n} \left((\Delta p_i/L)_{\text{pred}} - (\Delta p_i/L)_{\exp e} \right)^2} \tag{19}$$

The average percent error is a measure of the agreement between predicted and measured data. It indicates the degree of overprediction (positive values) or underprediction (negative values). Similarly, the average absolute percent error is a measure of the agreement between predicted and measured data. However, in this parameter the positive errors and the negative errors are not canceled. For this reason, the average absolute percent error is considered a key parameter in order to evaluate the prediction capability of a correlation. The standard deviation indicates how close the predictions are to the experimental data. The statistical parameters E_4, E_5 and E_6 are similar to E_1, E_2 and E_3 but the difference is that they are not based on the errors relative to the experimental pressure drop per unit length.

The minimum and maximum possible values for the PF are 0 and 6, corresponding to the best and the worst prediction performance, respectively.

The comparison of the accuracy of pressure gradient prediction of the correlations and the models from different authors against 2435 points is shown in Table 6. The measure of performance (PF) is a weighted measure using data from the columns E_1–E_6. The overall performance is given in the column PF; the smaller the number the more accurate is the prediction. The statistical parameters E_1–E_6 for each correlation or model are also included.

The performance of our correlation (9)–(12) sorted by flow pattern FFPC is best and the universal correlation FFUC given by (8) in which flow patterns are ignored is second best. In general, the Cicchitti et al. (1960) model presented extremely high errors, therefore, this model was not included in the performance factors evaluation (PF). However, we present the statistical parameters for comparison purposes.

It is of interest for applications to pipelines in reservoirs of heavy oil to evaluate predictors against high viscosity ($\mu_L \geqslant 400cP$) data; this is done in Table 7.

Table 6
Comparison of the accuracy of pressure gradient prediction of the correlations and the models from different authors against 2435 points

Model or correlation	PF	Statistical parameters					
		E_1 [%]	E_2 [%]	E_3 [%]	E_4 [Pa/m]	E_5 [Pa/m]	E_6 [Pa/m]
FFPC	0.02	−4.88	21.71	43.17	−72.58	316.11	805.05
FFUC	0.15	−5.78	24.61	46.76	−167.05	355.84	905.58
DUC	0.18	−6.86	24.85	58.03	−61.34	401.60	1025.78
PMM	0.32	−16.89	28.12	44.53	31.04	492.53	1232.89
OHM	0.57	−25.39	33.39	50.96	−266.56	438.04	1128.86
XMM	0.58	5.80	39.94	111.66	−139.94	474.20	1063.25
LMC	0.64	21.39	40.48	90.05	26.81	489.00	1386.80
BWHM	0.67	20.01	35.62	68.95	253.71	551.33	1402.55
MHM	0.82	−6.97	38.28	68.06	−598.92	686.35	1587.55
ORC	2.05	66.51	78.15	148.87	459.75	672.36	2374.55
OMM	3.22	95.74	137.33	326.82	−234.27	483.01	958.99
BBC	4.52	57.85	64.61	204.12	1893.18	1983.48	23 631.94
CHM	–	267.90	275.09	785.32	2253.64	2443.48	9717.73

Table 7
Comparison of the accuracy of pressure gradient prediction of the correlations and the models from different authors against high viscosity data ($\mu_L \geqslant 400cP$)

Model or correlation	PF	Statistical parameters					
		E_1 [%]	E_2 [%]	E_3 [%]	E_4 [Pa/m]	E_5 [Pa/m]	E_6 [Pa/m]
FFPC	0.19	−7.69	13.85	19.50	−324.70	548.52	1002.14
LMC	0.21	11.96	15.63	25.83	264.44	451.66	680.95
ORC	0.67	−15.66	17.06	23.71	−784.29	806.16	1558.81
PMM	0.87	−5.54	25.50	38.62	−67.51	1209.06	2098.29
XMM	0.93	−14.60	21.90	35.38	−774.55	919.34	1800.90
FFUC	0.99	−17.83	22.21	32.37	−839.13	990.39	1877.80
BBC	1.08	8.38	32.16	36.59	409.69	1431.56	1991.89
OMM	1.35	−24.84	25.70	37.79	−1139.83	1160.54	2133.75
OHM	1.37	−25.33	26.13	38.20	−1148.14	1168.21	2139.71
DUC	1.73	−33.28	34.32	45.78	−1215.72	1275.54	2299.17
BWHM	5.19	76.83	96.49	112.62	2788.11	3535.97	4419.79
MHM	5.69	−90.00	90.00	90.78	−4160.27	4160.27	5096.26
CHM	–	1039.61	1039.62	1924.47	25 161.28	25 162.36	40 687.65

The correlations FFPC which have been sorted by flow type again have the best performance, but the universal correlation falls to sixth place. As a practical matter, the flow of heavy oils in pipelines will be much slower than the flows of gas in mobile liquids like water. Turbulent flow which lead to dispersed bubble and annular flow do not typically occur in high viscosity fluids.

We turn now to an evaluation of the predictors when the experimental data is restricted by flow type. The following data were used: 1416 slug flow data points, 40 dispersed bubble data points,

689 stratified flow data points, and 249 annular flow data points. Forty-one data points corresponding to transitions were not considered in this evaluation. The PF and the statistical parameters for each flow pattern are presented in Tables 8–11. This kind of comparison naturally favors correlations like FFPC, which recognize the flow pattern. The excellent performance of FFUC, which does not recognize the flow pattern is noteworthy. For slug flow and stratified flow universal correlations may be recommended. The universal correlation also works well in the flow types of dispersed bubble and annular flow which are generated by turbulence.

Table 8
Evaluation of the correlations and the models using slug flow data

Model or correlation	PF	Statistical parameters					
		E_1 [%]	E_2 [%]	E_3 [%]	E_4 [Pa/m]	E_5 [Pa/m]	E_6 [Pa/m]
FFPC	0.05	−2.46	12.97	18.33	−64.40	356.30	806.01
FFUC	0.20	−4.71	13.34	18.48	−137.43	363.97	827.89
DUC	0.71	−2.55	18.23	29.67	98.13	456.02	1058.43
OHM	0.76	−10.81	16.73	23.77	−224.93	423.60	818.90
PMM	0.92	−4.90	17.64	24.90	245.20	566.03	1338.74
OMM	1.20	−16.14	20.56	27.25	−297.20	427.74	757.83
XMM	1.46	−8.76	21.05	42.94	−238.29	513.36	1052.57
LMC	1.95	5.13	25.89	52.58	−11.35	666.58	1750.58
ORC	2.02	10.67	22.72	41.60	428.59	644.56	1796.58
BWHM	2.21	16.17	25.60	44.80	346.31	635.02	1415.98
MHM	2.59	−19.51	26.09	36.16	−724.62	804.14	1579.15
BBC	6.00	33.94	37.23	62.40	1499.12	1526.97	4194.43
CHM	–	79.42	88.89	406.45	979.74	1276.93	3757.37

Table 9
Evaluation of the correlations and the models using dispersed bubble flow data

Model or correlation	PF	Statistical parameters					
		E_1 [%]	E_2 [%]	E_3 [%]	E_4 [Pa/m]	E_5 [Pa/m]	E_6 [Pa/m]
FFPC	0.27	−3.37	8.30	12.56	−144.79	268.42	558.73
LMC	0.29	−0.26	10.91	15.82	84.06	235.19	344.78
DUC	0.38	−2.31	10.88	15.88	−22.77	267.14	430.77
FFUC	0.45	−4.57	8.99	13.22	−187.76	318.66	608.44
ORC	0.90	−9.56	9.94	15.99	−328.58	338.39	638.78
PMM	0.95	−4.97	12.34	17.04	94.60	528.37	898.92
OHM	1.10	−10.49	11.06	16.14	−388.11	396.46	743.57
OMM	1.11	−10.53	11.17	16.25	−388.51	397.38	743.75
BWHM	1.98	−1.56	17.55	23.91	467.03	863.05	1622.44
XMM	2.50	−19.66	19.69	25.28	−562.37	566.07	863.44
BBC	3.05	16.11	21.89	26.40	829.93	913.49	1425.16
MHM	6.00	−25.82	26.55	40.81	−1817.96	1833.17	3672.19
CHM	–	−5.10	11.68	16.83	54.46	485.54	854.94

Table 10
Evaluation of the correlations and the models using stratified flow data

Model or correlation	PF	Statistical parameters					
		E_1 [%]	E_2 [%]	E_3 [%]	E_4 [Pa/m]	E_5 [Pa/m]	E_6 [Pa/m]
FFUC	0.08	2.62	42.26	78.62	−28.04	65.24	169.81
FFPC	0.19	−7.06	37.73	73.78	−42.75	63.59	184.64
BWHM	0.25	38.97	55.34	107.53	31.59	63.65	155.69
DUC	0.44	−6.91	36.22	97.13	−53.81	73.97	221.44
PMM	0.52	−30.75	41.34	66.60	−63.80	78.27	212.20
MHM	0.56	31.04	62.80	112.01	−32.82	83.33	246.61
OHM	0.78	−42.72	56.81	77.77	−83.33	89.73	203.98
LMC	0.92	61.77	76.22	149.44	63.66	95.66	207.92
XMM	1.44	18.56	62.27	163.87	65.31	129.15	415.84
BBC	2.57	86.93	98.53	155.14	120.56	149.97	591.11
ORC	3.54	175.05	185.76	260.63	177.07	207.82	445.12
OMM	5.59	375.68	408.47	607.19	167.69	285.88	438.02
CHM	–	567.25	571.32	1167.78	1255.75	1260.07	5452.57

Table 11
Evaluation of the correlations and the models using annular flow data

Model or correlation	PF	Statistical parameters					
		E_1 [%]	E_2 [%]	E_3 [%]	E_4 [Pa/m]	E_5 [Pa/m]	E_6 [Pa/m]
LMC	0.04	5.86	32.32	40.13	40.77	579.49	1034.69
FFPC	0.07	−10.95	29.60	33.95	−92.04	712.72	1476.08
BWHM	0.20	−14.36	34.86	40.92	−154.76	941.65	2023.93
DUC	0.35	−27.89	32.02	38.61	−830.31	903.96	1753.62
MHM	0.40	−27.65	36.13	43.74	−758.63	1005.23	2058.40
FFUC	0.50	−33.33	43.01	47.20	−621.68	1031.67	1899.61
PMM	0.83	−52.37	54.09	58.04	−1041.83	1121.24	1983.01
OMM	0.94	−6.06	90.20	145.26	−849.44	1280.14	2163.31
OHM	1.10	−63.01	68.26	72.79	−882.19	1401.13	2832.41
XMM	1.40	61.07	92.47	192.75	−5.03	1161.30	1981.09
ORC	2.25	108.83	115.76	137.80	1727.84	2127.30	5987.36
BBC	6.00	126.90	139.72	565.21	9398.50	9973.73	73 340.33
CHM	–	432.36	434.45	841.23	9279.49	9359.79	23 612.58

6. Summary and conclusions

Data from 2435 gas–liquid flow experiments in horizontal pipelines were sorted by flow pattern and a data structure suitable for the construction of correlations of friction factor vs. Reynolds number was created.

A mixture friction factor (1) and mixture Reynolds number (4) were selected to reduce the scatter of the data. The Reynolds number is based on the mixture velocity and the liquid kinematic viscosity; the frictional resistance of the liquid is most important.

Data from 2060 of the 2435 experiments were processed for power law correlation in log–log plots of friction factor vs. Reynolds number.

Power laws for laminar and turbulent gas–liquid flow were determined for all 2060 points irrespective of flow patterns; we called such correlations, which are independent of flow type, universal.

Power laws for laminar and turbulent gas–liquid flow were determined for subsets of the 2060 points corresponding to stratified, slug, disperse bubble and annular flow. The experiments and prefactors for the power laws for gas–liquid flows can be compared to those for single phase flows. In fact, there is a similarity between the two- and single-phase cases when the Reynolds numbers are small (laminar) and large (turbulent). In the laminar case the friction factors are not so very different than the single phase $16/Re$, independent of flow type. In the turbulent case the Blasius exponent -0.25 for a single phase can be compared to exponents ranging from -0.1225 for annular flow to -0.263 for slug and dispersed flow. The flow resistance for slug and dispersed flow patterns is dominated by the frictional resistance of the liquid on the wall. For stratified and annular flow the gas flows through an open channel, not blocked by liquid, and at large Reynolds numbers the gas flow is turbulent. The size of this open channel is not given in this correlation; it is possible that the turbulent gas which determines the frictional resistance, follows the Blasius law when the effective channel size (given by the gas hold-up) is known. On the other hand, an increase in frictional resistance from atomization and effective roughness due to waves on the water also plays a role. The variations of the exponent in turbulent flow presents a challenge for future research.

The transition region going from laminar to turbulent flow was fit to a logistic dose curve. This fitting procedure leads to rational fractions of power laws which reduce to laminar flow at small Reynolds number and to turbulent flow at large Reynolds number. We call these rational fraction of power laws composite; one formula for all Reynolds numbers. Composite power laws are very practical because the transition region is predicted to a statistical accuracy consistent with spread of the data.

The predictions of the composite correlations were tested internally for the spread of the actual data against the predictions. The same tests were carried out for the correlations sorted by flow type. The standard deviations are small for slug flow, which is main flow type of viscous oils, and bubble flow which requires turbulent flow with a relatively small gas fraction.

The prediction of the composite correlations were tested externally against correlations, homogeneous models and mechanistic models from the literature. The composite correlations sorted by flow type are more accurate than any other predictor for all cases except stratified and annular flows. The universal composite correlation is the most accurate in stratified flow. The Lockhart and Martinelli (1949) correlation shows the best performance in annular flow. However, our correlation for annular flow has the least average absolute percent error. The universal composite correlation is second best in the data set in which all flow types are included, followed in third place by the Dukler et al. (1964) correlation. When sorted by viscosity, the Dukler correlation falls to tenth place. Slug flow is the main flow type in the data set for high viscosity liquid (42.74% points) and the composite correlation for slug flow may be recommended. In general, the Cicchitti et al. (1960) model has the biggest errors.

In annular and stratified flow the effect of the relative velocity of the phases, neglected in this paper, should be significant. Including the hold-up, as was done by Mata et al. (2002), could give rise to improved correlations.

Universal (independent of flow type) and composite (for all Reynolds numbers) correlations are very useful for field operations for which the flow type may not be known. It is a best guess for the pressure gradient when the flow type is unknown or different flow types are encountered in one line.

A dimensionless pipe roughness is given in the database and ranges from smooth (41% points) to rough (59% points) pipes. The data and correlations for two-phase turbulent flow in pipes do not appear to depend strongly on pipe roughness; "effective" roughness arises from the action of natural fluctuations of one-phase on another. This needs further study.

Acknowledgements

The authors would like to thank to A. Brito and J. Colmenares for their contributions in the Intevep's data collection. F. García would like to acknowledge the CDCH-UCV, Escuela de Ingeniería Mecánica de la Universidad Central de Venezuela and PDVSA-Intevep for supporting his Doctoral Study. The work of D.D. Joseph was supported by PDVSA-Intevep and the Engineering Research Program of the Office of Basic Energy Sciences at the DOE, and under an NSF/GOALI grant from the division of Chemical Transport Systems.

References

Agrawal, S., 1971. Horizontal two phase stratified flow in pipe, M.Sc. Thesis, University of Calgary.

Alves, G., 1954. Concurrent liquid–gas flow in a pipe-line contactor. Chem. Eng. Prog. 50, 449–456.

Andritsos, N., 1986. Effect of pipe diameter and liquid viscosity on horizontal stratified flow, Ph.D. Dissertation, University of Illinois at Champaign-Urbana.

Ansari, A., Sylvester, N., Sarica, C., Shoham, O., Brill, J., 1994. A Comprehensive Mechanistic Model for Upward Two-Phase Flow in Wellbores. SPE Prod. Facilities J., 142–152.

Aziz, K., Gregory, G., Nicholson, M., 1974. Some observation on the motion of elongated bubbles in horizontal pipes. Can. J. Chem. Eng. 52, 695–702.

Beattie, D., Whalley, P., 1982. A simple two-phase frictional pressure drop calculation method. Int. J. Multiphase Flow, 83–87.

Beggs, H., 1972. An experimental study of two-phase flow in inclined pipes, Ph.D. Dissertation, University of Tulsa.

Beggs, H., Brill, J., 1973. A study of two phase flow in inclined pipes. J. Pet. Technol. 25, 607–617.

Cabello, R., Cárdenas, C., Lombano, G., Ortega, P., Brito, A., Trallero, J., Colmenares, J., 2001. Pruebas Experimentales con Kerosén/Aire para el Estudio de Flujo Tapón con Sensores Capacitivos en una Tubería Horizontal, INT-8898-2001. PDVSA INTEVEP, 50 p.

Cheremisinoff, N., 1977. An experimental and theoretical investigation of horizontal stratified and annular two phase flow with heat transfer, Ph.D. Dissertation, Clarkson College of Technology.

Chisholm, D., 1967. A theoretical basis for the Lockhart–Martinelli correlation for two-phase flow. Int. J. Heat Mass Transfer 10, 1767–1778.

Cicchitti, A., Lombardi, C., Silvestri, M., Soldaini, G., Zavattareui, R., 1960. Two-phase cooling experiments—pressure drop, heat transfer and burnout measurements. Energy Nucl. 7, 407–425.

Dukler, A., Wicks III, M., Cleveland, R., 1964. Frictional pressure drop in two-phase flow: B. An approach through similarity analysis. AIChE J. 10, 44–51.

Eaton, B., 1966. The prediction of flow patterns, liquid holdup and pressure losses occurring during continuous two-phase flow in horizontal pipelines, Ph.D. Thesis, University of Texas, 169 p.

Govier, G., Omer, M., 1962. The horizontal pipeline flow of air–water mixture. Can. J. Chem. Eng. 40, 93.

Joseph, D.D., 2002. Interrogations of direct numerical simulation of solid–liquid flow. Published by eFluids.com, <http://www.efluids.com/books/joseph.htm>.

Kokal, S., 1987. An experimental study of two-phase flow in inclined pipes, Ph.D. Dissertation, University of Calgary, Alberta, Canada.

Lockhart, R., Martinelli, R., 1949. Proposed correlation of data for isothermal two-phase two component flow in pipes. Chem. Eng. Prog. 45, 39–48.

Mata, C., Vielma, J., Joseph, D., 2002. Power law correlations for gas/liquid flow in a flexible pipeline simulating terrain variation. Int. J. Multiphase Flow, submitted for publication. Also see <http://www.aem.umn.edu/people/faculty/joseph/PL-correlations/docs-ln/PLC-FlexPipe.pdf>.

Mattar, L., 1973. Slug flow uphill in an inclined pipe, M.Sc. Thesis, University of Calgary.

McAdams, W., Woods, W., Heroman, L., 1942. Vaporization inside horizontal tubes. Trans. ASME 64, 193.

Mukherjee, H., 1979. An experimental study of iTwo-phase flow, Ph.D. Dissertation, University of Tulsa.

Oballa, V., Coombe, D., Buchanan, W., 1997. Aspects of discretized Wellbore modelling coupled to compositional/thermal simulation. JCPT 36, 45–51.

Ortega, P., Trallero, J., Colmenares, J., Brito, A., Cabello, R., González, P., 2001. Experimentos y Validación de Modelo para Predicción del Gradiente de Presión de Flujo Tapón en Tuberías Horizontales para un Sistema Bifásico Altamente Viscoso Aceite (1200 cP)/Aire, INT-8879-2001. PDVSA INTEVEP, 37 p.

Ortega, P., Trallero, J., Colmenares, J., Cabello, R., González, P., 2000. Modelo para la Predicción de la Caáda de Presión en Flujo Tapón para una Tubería Horizontal. INT-8123-2000. PDVSA INTEVEP, 19 p.

Ouyang, L., 1998. Single phase and multiphase fluid flow in horizontal wells, Ph.D. Dissertation Thesis, Department of Petroleum Engineering, School of Earth Sciences, Stanford University. Stanford, CA, 248 p.

Padrino, J., Pereyra, E., Brito, A., Garcia, F., Cardozo, M., Ortega, P., Colmenares, J., Trallero, J., 2002. Modelo para la Predicción del Gradiente de Presión en Pozos y Tuberías Horizontales—Parte I, INT-9508-2002. PDVSA INTEVEP, 141 p.

Pan, T., Joseph, D., Bai, R., Glowinski, R., Sarin, V., 2002. Fluidization of 1204 spheres: simulation and experiment. J. Fluid Mech. 451, 169–191.

Patankar, N., Huang, P., Ko, T., Joseph, D., 2001a. Lift-off of a single particle in Newtonian and viscoelastic fluids by direct numerical simulation. J. Fluid Mech. 438, 67–100.

Patankar, N., Ko, T., Choi, H., Joseph, D., 2001b. A correlation for the lift-off of many particles in plane Poiseuille flows of Newtonian fluids. J. Fluid Mech. 445, 55–76.

Patankar, N., Joseph, D., Wang, J., Barree, R., Conway, M., Asadi, M., 2002. Power law correlations for sediment transport in pressure driven channel flows. Int. J. Multiphase Flow 28, 1269–1292.

Pereyra, E., Ortega, P., Trallero, J., Colmenares, J., 2001. Validación del Modelo Mecanicista de Gradiente de Presión para Flujo Tapón en un Sistema Crudo/Gas, INT-8894-2001. PDVSA INTEVEP, 48 p.

Rivero, M., Laya, A., Ocando, D., 1995. Experimental study on the stratified-slug transition for gas–viscous liquid flow in horizontal pipelines. BHR Group Conf. Ser. Publ. 14, 293–304.

Viana, F., Pardo, R., Yánez, R., Trallero, J., Joseph, D., 2003. Universal correlation for the rise velocity of long gas bubbles in round pipes, J. Fluid Mech., accepted for publication.

Wang, J., Joseph, D., Patankar, N., Conway, M., Barree, B., 2002. Bi-power law correlations for sedimentation transport in pressure driven channel flows. Int. J. Multiphase Flow 29, 475–494.

Xiao, J., Shoham, O., Brill, J., 1990. A comprehensive model for two-phase flow in pipelines. In: The 65th SPE Annual Technical Conference and Exhibition, New Orleans, LA, September 23–26. SPE 20631. pp. 167–180.

Yu, C., 1972. Horizontal flow of air–oil mixtures in the elongated bubble flow pattern, M.Sc. Thesis, University of Calgary.